

## Nanochemistry and technology

---

Simulation of surface acoustofluidic wave  
(SAW) initiated particle controlling in the  
application of polymer particle manipulation

---

Keer ZHANG

Academic year 2019-2020

# Contents

1	Introduction . . . . .	2
2	Theoretical description . . . . .	3
3	Simulation with COMSOL Multiphysics® . . . . .	5
3.1	SAW pressure field generation . . . . .	7
3.2	Particle movement . . . . .	8
4	Conclusion . . . . .	12
	<b>Bibliography</b>	<b>13</b>

# 1 Introduction

The aim of this project is to study the application of acoustofluidics in the field of particle manipulation.

In general this method can be classified into two distinct subcategories based the force involved, being acoustic radiation and acoustic streaming[1] respectively. The radiation force, which results from scattering of sound wave on the particles[2], can in turn move particles to the pressure nodes or antinodes based on compressibility and density of both particle itself and fluid media[3]. The streaming force, on the other hand, arises from the viscous attenuation of fluid and can drag particles along the streaming flow induced by acoustic field[1, 3].

Bulk acoustic wave (BAW) and surface acoustic wave (SAW) are two typically types of acoustic waves that are used for particle manipulation[4]. In the case of BAW-based device, a pair of interdigitated transducers (IDT) is bound to a fluid chamber made of materials with high acoustic impedance such as glass and stainless steel, so that the induced acoustic wave can be perfectly reflected on the channel wall[5, 3]. The wavelength is controlled by the depth and width of the channel. SAW, on the other hand, is generated by two pairs of IDT placed opposite to each other. The interference of two counter-propagating waves will create a standing SAW in between of two IDTs[3]. In the case of SAW, the wavelngth is controlled by the distance between IDT and channel when IDT properties are fixed.

This study focuses on the manipulation of polymer particles by SAW through acoustic radiation force. First a brief description of the theories involved in SAW-radiation-force-based particle manipulation is given, followed by the simulation of the process with COMSOL Multiphysics®.

## 2 Theoretical description

The acoustic force on particle is given by[3, 5]:

$$F_R = -(\frac{\pi p_0^2 V_p \beta_f}{2\lambda})\phi(\beta, \rho)\sin(\frac{4\pi x}{\lambda}) \quad (1)$$

$$\phi(\beta, \rho) = \frac{5\rho_p - \rho_f}{2\rho_p + \rho_f} - \frac{\beta_p}{\beta_f} \quad (2)$$

with

- $p_0$ : acoustic pressure
- $V_p$ : volume of particle
- $\beta_f$ : compressibility of the fluid
- $\beta_p$ : compressibility of the particle
- $\rho_f$ : density of the fluid
- $\rho_p$ : density of the particle
- $\phi$ : acoustic contrast factor
- $\lambda$ : wavelength of the acoustic wave
- $x$ : distance from a pressure node

When  $\phi > 0$ , the object will move towards pressure nodes, otherwise it will move towards antinodes. Eq. 1 also implies the dependency of acoustic radiation force on particle volume. As is indicated in the equation, a bigger volume can result in a higher radiation force when particle material and external acoustic field are fixed. Hence, there will be a critical size of the particle below which the manipulation by acoustic radiation force will be hard or even unfeasible.

To manipulate particles with SAW, a channel, typically made of PMMA, is first placed in between two IDTs which continuously generate waves so as to create a pressure field. Laminar flow is constantly pumped into the channel with a fixed velocity, while the flow profile is both spatially and temporally unchanged. Particles carried by the flow will experience the effect of acoustic pressure field and flow towards pressure nodes or antinodes. The

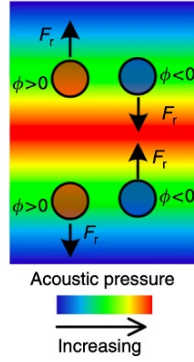


**Figure 1: Movements of particles in acoustic pressure field[3]**

movement of particles can therefore be manipulated.

In this study, polystyrene (PS) particle is selected as the particles that will be monitored, while water is chosen to be the fluid medium. The compressibility and density of both components are listed in Table 1. By doing the calculation with Eq. 2,  $\phi$  can be calculated,

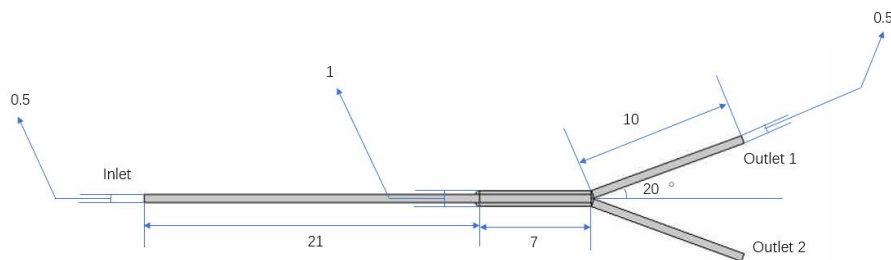
	PS	Water
Compressibility (1/Pa)	$2.46 \times 10^{-10}$	$4.58 \times 10^{-10}$
Density (g/cm <sup>3</sup> )	1.05	1.00

**Table 1: Compressibility and density of water and PS**

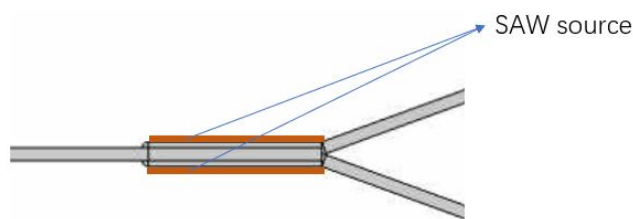
which equals to 0.511. This result indicates that PS particles will move towards pressure nodes when being placed in SAW field.

### 3 Simulation with COMSOL Multiphysics®

In order to simulate the movement of PS particle in SAW field, first, a Y-shape channel is built based on the typical design of channel from literature[3, 4, 6, 7]. The schematic of the channel is presented in Figure 2(a). Additionally, 'Plane wave radiation' nodes are added on both sides of the channel to simulate the wave generated by IDTs, as is indicated in Figure 2(b). The channel has one inlet and two outlets, with the inlet being placed on the left and



(a)

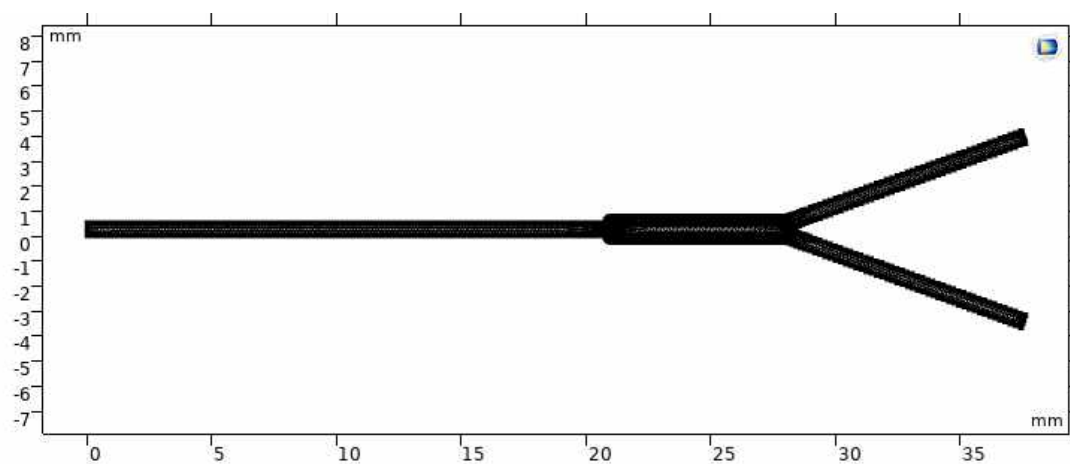


(b)

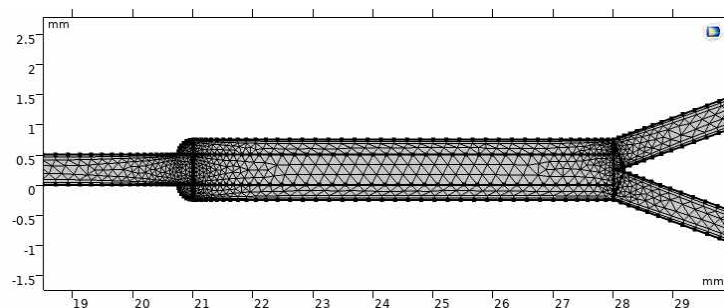
**Figure 2: (a)Schematic of the channel. The channel is perfectly symmetrical with regarding to the central horizontal line. All values (except already indicated in the figure) are in mm. (b)Location of SAW source**

two outlets being placed on the right, respectively. Ideally, the manipulation should take place in the part indicated in Figure 2(b).

The mesh is presented in Figure 3(a), with its quality selected to be 'Fine' since both simulation quality and computation time are considered. The part where separation is supposed to take place (the part represented by Figure 2(b)) is presented in Figure 3(b).



(a)



(b)

Figure 3: Mesh (a)whole channel (b)Part where manipulation takes place

### 3.1 SAW pressure field generation

The first step of the simulation is to generate a pressure field based on the simulation using 'Pressure Acoustic, Frequency Domain' node in water. The pressure amplitude is selected to be 100kPa based on the literature[7]. The phase angle difference between two waves is  $\pi/2$ . In order to find a proper frequency so that the manipulation behavior can be easily assessed, ideally the part where manipulation takes place should have one pressure node and one antinode, each located at the entrance of two outlets so that the ratio of collected particles at one outlet can represent the quality of manipulation. Hence, a parametric sweep study of the applied frequency being in the range of 1MHz and 10MHz is first performed, as is presented in Figure 4. It can be concluded that the density of pressure nodes and antinodes

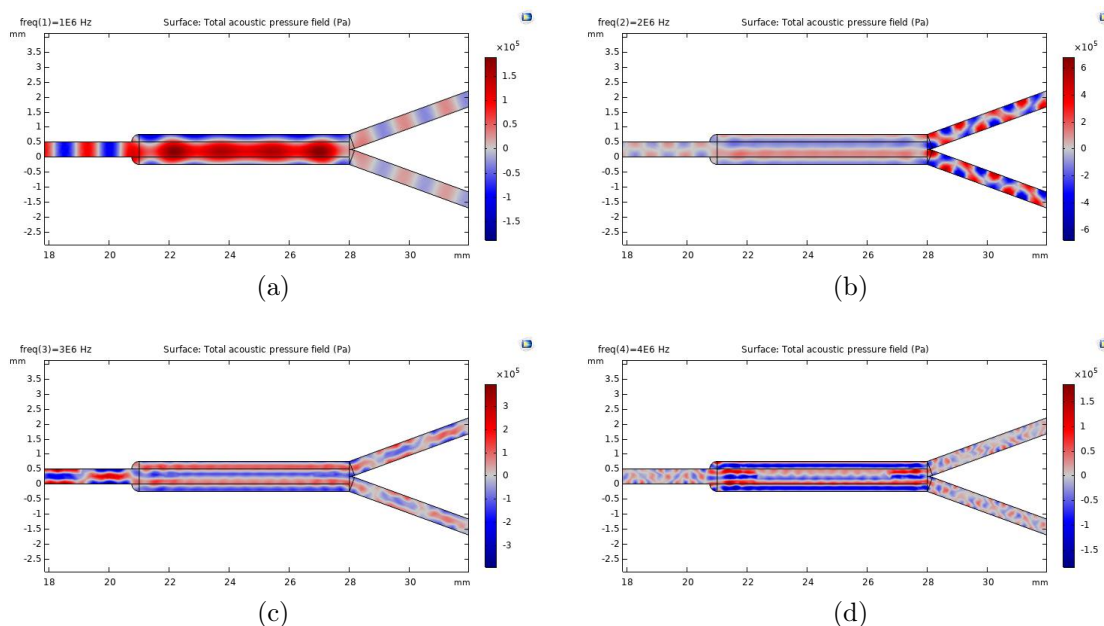


**Figure 4: Pressure field at frequency being (a)1MHz (b)2MHz (c)3MHz (d)4MHz. Color bar represents acoustic pressure intensity.**

increases with frequency, and the optimal frequency is in between 1MHz and 2MHz where distribution of pressure nodes and antinodes agree with the description at the beginning of this section. Hence, another parametric study of frequency with value being in the range from 1MHz to 2MHz is performed, as is presented in Figure 5. Based on the previous discussion, the frequency is selected to be 1.9MHz. In this case manipulation quality can be represented by the ratio of PS particles being collected at outlet 1. This is because  $\phi$  of PS is bigger than 0, therefore particles will move towards pressure nodes.



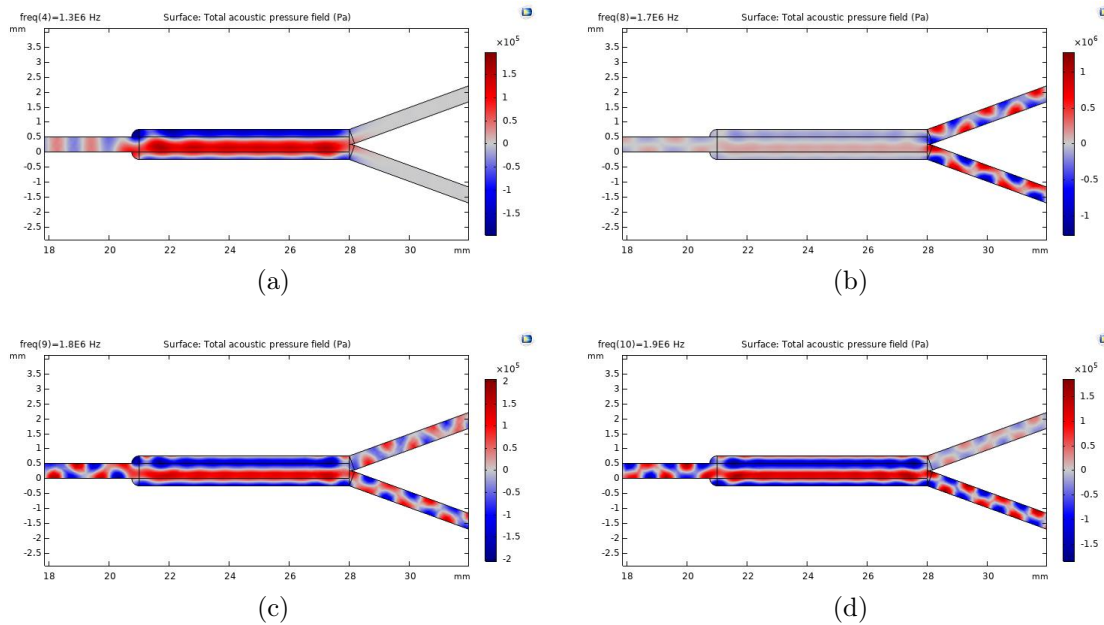


**Figure 5: Pressure field at frequency being (a)1.3MHz (b)1.7MHz (c)1.8MHz (d)1.9MHz. Color bar represents acoustic pressure intensity.**

### 3.2 Particle movement

In order to simulate the movement of particles, two nodes, being 'Laminar Flow' and 'Particle Tracing for Fluid Flow' are coupled together so that the carrying of particles by flow can be simulated. The inlet flow velocity is 5mm/s and is constant with time. 70 mono-dispersed particles are released at the inlet of the channel and their transmission probability are evaluated at both outlets.

Flow velocity profile is presented in Figure 6, indicating that the structure works well and flow can pass through both outlets with the same velocity profile. In order to assess the effect of particle size on manipulation, another parametric sweep study of particle size is performed, with particle diameter ranging from 2 microns to 10 microns being studied, and step is 2 microns. At the outlets the transmission probability is evaluated under 'Derived Values' in 'Results' node. A typical particle position profile with respect to time is presented in Figure 7.

The transmission probability with respect to time in this case is plotted in Figure 8, while the final transmission probability is 91.304% for the outlet 1 and 8.696% for outlet 2.

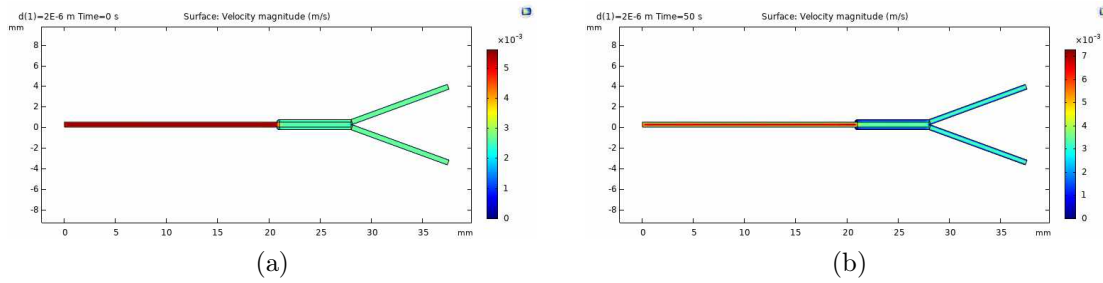


Figure 6: Velocity profile at (a) 0s (b) 50s. Color bar represents flow velocity.

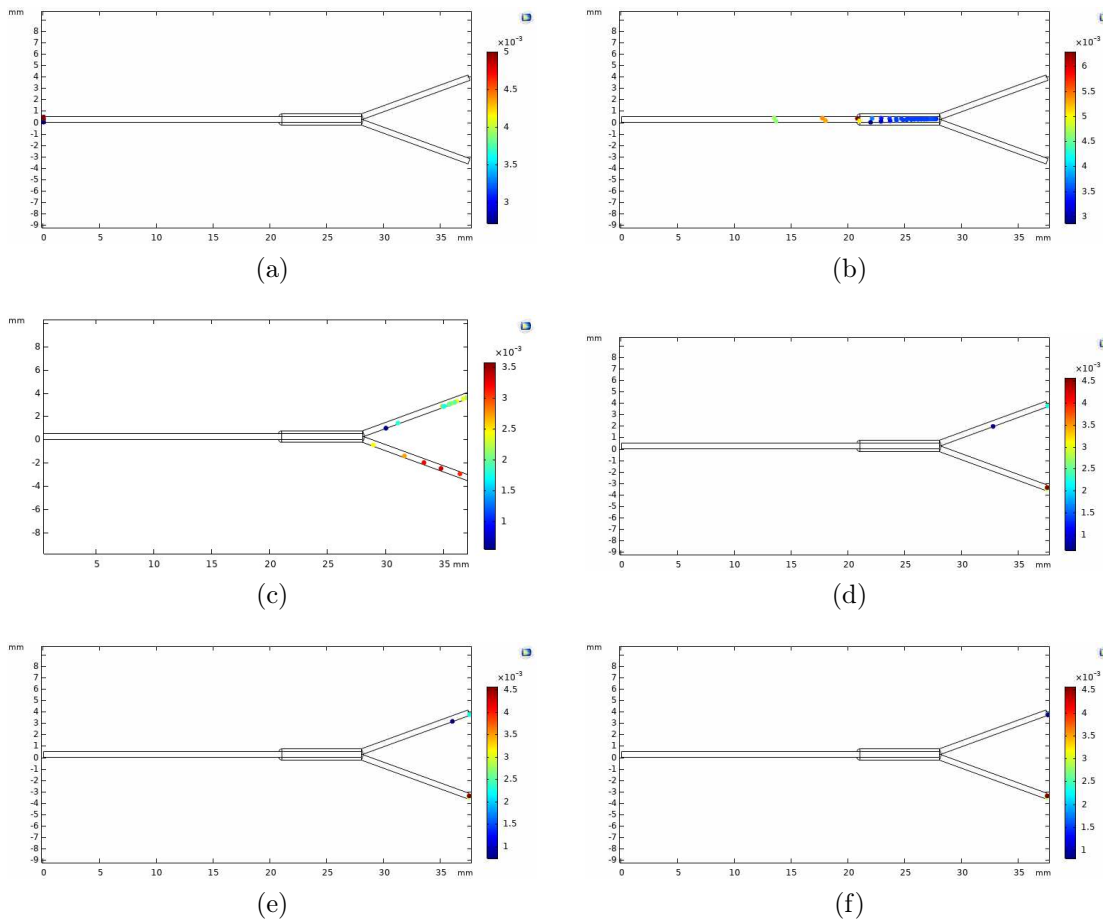


Figure 7: Particle position profile with respect to time at  $t$  being (a) 0s (b) 5s (c) 10s (d) 15s (e) 20s (f) 50s when particle diameter is 10 microns. Color bar represents particle velocity.

The transmission probability for different size of particles at both outlets is presented in Table 2. The results are also presented graphically in Figure 9. The fact that sum of trans-

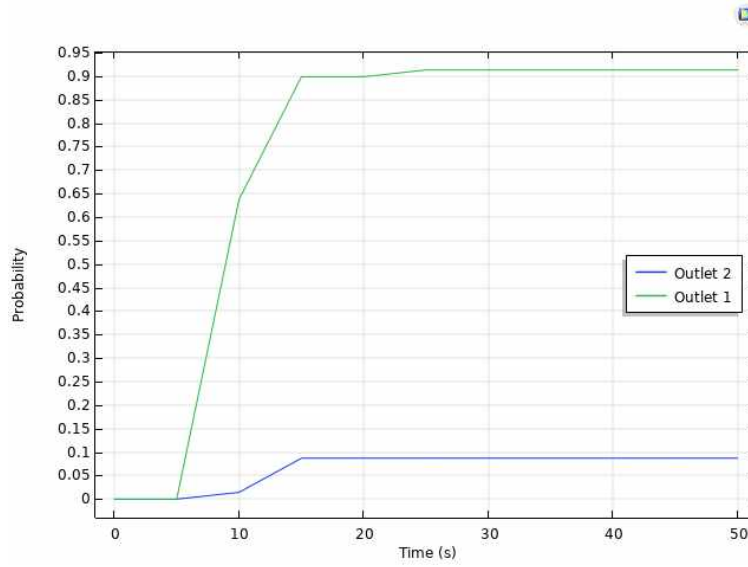


Figure 8: Transmission probability at both outlets with respect to time when particle diameter is  $10\mu m$ .

	Outlet 1	Outlet 2
$2\mu m$	54.286%	45.714%
$4\mu m$	51.471%	48.529%
$6\mu m$	69.565%	30.435%
$8\mu m$	76.119%	23.881%
$10\mu m$	91.304%	8.696%

Table 2: Transmission probability at both outlets. Maximum:  $10\mu m$  Minimum:  $2\mu m$  Step:  $2\mu m$

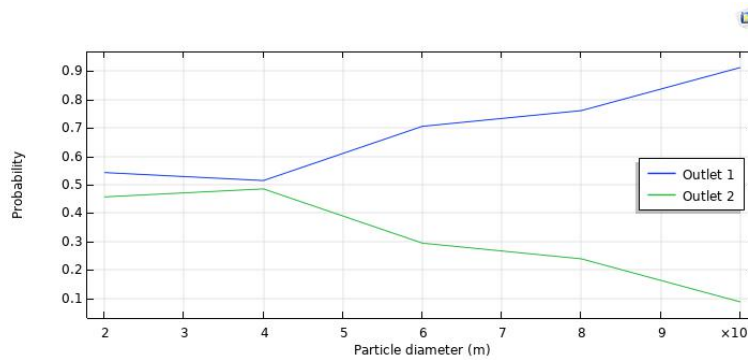
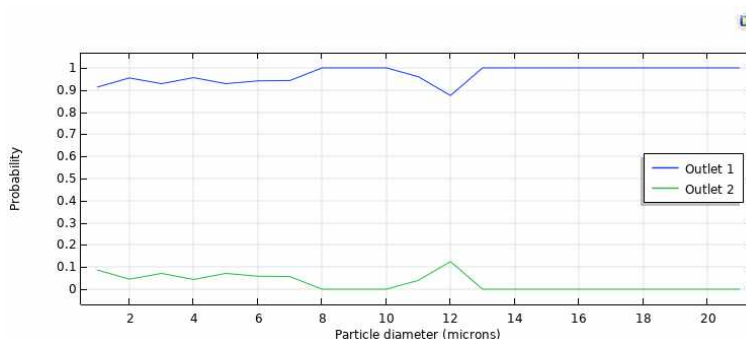


Figure 9: Transmission probability at both outlets with respect to particle diameter. Maximum:  $10\mu m$  Minimum:  $2\mu m$  Step:  $2\mu m$

mission probability always equals to 1 at both outlets when particle diameter is fixed implies that all particles have been collected at either outlet 1 or outlet 2 at  $t=50s$ . In general, the transmission probability at outlet 1 increases with particle diameter, which agrees with the theory.

Another parametric sweep study is performed to find the critical particle diameter of which all the particles can be collected at outlet 1. As is indicated in Table 9 and Figure 10, the critical diameter is around  $11.2\ \mu m$ .



**Figure 10: Transmission probability at both outlets with respect to particle diameter. Maximum:  $12\mu m$  Minimum:  $10\mu m$  Step:  $0.1\ \mu m$**

## 4 Conclusion

This work has investigated into SAW assisted particle manipulation. Based on the discussion in the theoretical part, it is expected that the manipulation behavior is greatly influenced by particle size when other properties are fixed. Simulation performed with COMSOL Multiphysics® has demonstrated this conclusion, showing that the probability of PS particles moving towards the pressure node and being collected at outlet 1 increases with particle diameter. It is also found that when particle diameter reaches around  $11.2\ \mu m$ , the transmission probability of particles being collected at outlet 1 will reach 100%, indicating that all the particles can be manipulated as required. Further application of this technique in the fields like liquid purification, particle separation and droplet manipulation is quite promising.

# Bibliography

- [1] Philipp Hahn, Ivo Leibacher, Thierry Baasch, and Jurg Dual. Numerical simulation of acoustofluidic manipulation by radiation forces and acoustic streaming for complex particles. *Lab Chip*, 15:4302–4313, 2015.
- [2] Peter Barkholt Muller, Rune Barnkob, Mads Jakob Herring Jensen, and Henrik Bruus. A numerical study of microparticle acoustophoresis driven by acoustic radiation forces and streaming-induced drag forces. *Lab on a Chip*, 12(22):4617–4627, 2012.
- [3] Mengxi Wu, Adem Ozcelik, Joseph Rufo, Zeyu Wang, Rui Fang, and Tony Jun Huang. Acoustofluidic separation of cells and particles. *Microsystems & nanoengineering*, 5(1):32, 2019.
- [4] Zhichao Ma, David J Collins, and Ye Ai. Detachable acoustofluidic system for particle separation via a traveling surface acoustic wave. *Analytical chemistry*, 88(10):5316–5323, 2016.
- [5] Yuchao Chen, Mengxi Wu, Liqiang Ren, Jiayang Liu, Pamela H Whitley, Lin Wang, and Tony Jun Huang. High-throughput acoustic separation of platelets from whole blood. *Lab on a Chip*, 16(18):3466–3472, 2016.
- [6] Zezheng Wu, Hongqiang Jiang, Lingling Zhang, Kezhen Yi, Heng Cui, Fubing Wang, Wei Liu, Xingzhong Zhao, Fuling Zhou, and Shishang Guo. The acoustofluidic focusing and separation of rare tumor cells using transparent lithium niobate transducers. *Lab on a Chip*, 19(23):3922–3930, 2019.
- [7] Shivaraman Asoda. Simulation and optimization of a sheathless size-based acoustic particle separator. *University of South Florida Scholar commons: Graduate Theses and Dissertations*, 2018.